Iraqi Journal of Physics, 2026
https://doi.org/10.30723/ijp.v24i3.1586
Vol.24, No.3, PP.159-168
P-ISSN: 2070-4003
E-ISSN: 2664-5548

The M33 Cluster System: Fossil Records of a Galaxy's Evolution

Ahmed H. Abdullah[1*], Rasha H. Ibrahim[1], and Israa A. Mohammed Ali[2]
[1]*Department of Astronomy and Space, College of Science, University of Baghdad, Baghdad, Iraq*
[2]*Department of Remote Sensing, College of Remote Sensing and Geophysics, Al-Karkh University of Science, Baghdad, Iraq*
[*]Corresponding author: ahmed.h.abdullah@sc.uobaghdad.edu.iq

Abstract
This study uses star clusters of the Triangulum galaxy (M33) as fossil records to trace its evolutionary history. We synthesize previous observational studies of the cluster system's population, kinematics, and chemical properties to construct a unified evolutionary picture. The cluster system (GS) shows a clear age-metallicity relation (AMR), with younger clusters more metal-rich and metallicity dispersion increasing with age. The age distribution shows a prominent peak at approximately 10 Myr, indicating a distinct period of cluster formation. An age-velocity relation (AVR) is also observed, as random cluster velocities increase with age, reflecting progressive disk heating. The radial metallicity gradients evolve significantly over time: young clusters (< 150 Myr) exhibit a positive or nearly flat gradient of approximately +0.033 dex/kpc, intermediate-age clusters (1-4 Gyr) show a negative gradient of -0.036 dex/kpc, and older clusters > 4 Gyr within a radius of 4.5 kpc display a steeper negative gradient of -0.065 dex/kpc. These trends support an inside-out growth scenario for the M33 disk. Comparisons with other galaxies show that M33 resembles the Large Magellanic Cloud (LMC) in fraction of old clusters and mean cluster mass but differs from M31 and the Milky Way. Overall, the M33 cluster system preserves valuable fossil evidence of the galaxy's chemical, kinematic, and structural evolution.

Article Info.

Keywords:
Satellite Galaxies, Metallicity, Stellar Mass, Triangulum Galaxy, Cluster System.

Article history:
Received: Apr. 12, 2026
Revised: Jun. 02, 2026
Accepted: Jun. 22, 2026
Published:Sep. 01,2026

1. Introduction
Stellar clusters are among the most important tools for understanding galaxy evolution, preserving integrated-light records of the physical and chemical conditions present when they formed. As noted by [1-3], stellar clusters provide a crucial link between small star formation scales (individual star scales) and large scales (entire galaxies). Triangulum Galaxy (M33), the third member of the Local Group after the Andromeda Galaxy (M31) and the Milky Way (MW), is an ideal laboratory for studying the evolution of medium-mass spiral galaxies. M33 is located at a distance of 847 ± 60 kpc [4] with an inclination angle of i = 56º +/- 1º [5-6]. This makes it ideal for observational studies. Despite great efforts to study stellar clusters of M33, previous studies have used different methodologies and obtained different results. Several studies from [7-10] adopted the optical range only (3800-10000 Aº). This led to difficulty in separating the age-extinction degeneracy by using the spectral energy distributions (SED) [11]. While presenting a comprehensive catalog of 451 sources, including 255 confirmed clusters [12, 13] used data from ultraviolet to infrared clusters (GALEX FUV and NUV, UBVRI, Hα, and Spitzer 24μm) to perform SED fitting for 137 clusters. This study highlighted the age-extinction problem, showing that old, low-extinction clusters can be misinterpreted as high-extinction young clusters. The model form assumes a fixed metallicity, Z = 0.02 [14, 15]. Optical measurements for 708 candidates in M33 were provided by [16] using LGGS images [17]. This study showed that only 30.55% of clusters are older than 2 Gyr, indicating that M33 is dominated by young clusters smaller than 1 Gyr. The 30.55% value reported by [16] refers to their original sample only. The 16% in this work was derived from the final synthesized sample after the combination and cross-matching of the three datasets [18]. Provided high-resolution spectroscopic measurements for 77 clusters using the GTC (OSIRIS) and WHT

(WYFFOS/AF2) telescopes. This allowed for high-resolution determination of ages, metallicities, and radial velocities. This study showed a clear relationship between age and velocity dispersion, and revealed 12 globular clusters in M33.

This study is important because it uses the M33 star clusters as fossil records to track the galaxy's evolutionary history, so as to fill in the lack of a unified framework that integrates previous heterogeneous observational findings. Fig. 1 illustrates the age-extinction degeneracy, showing that clusters with high values of E(B−V) tend to have smaller ages in SED fitting solutions, reflecting the difficulty of separating these two parameters using only optical data. This study aims to provide a unified picture of the properties of stellar clusters in M33, focusing on: (1) age-metallicity relation (AMR), (2) age and metallicity distribution, (3) spatial and kinematic distribution, (4) the frequency evolution of radial metallicity, (5) comparison of the star clusters in M33 with other galaxies.

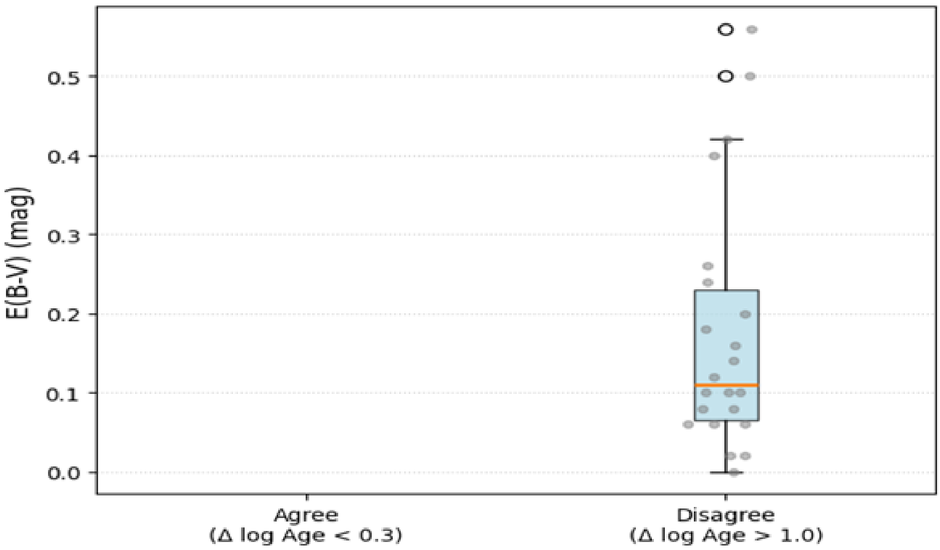

Figure 1: The age-extinction ratio in the spectral distribution structure of stellar clusters SED fitting Data from [13].

2. Data and Methodology

This study synthesizes data from three major complementary studies. First, the Moeller et al. [13] study used GALEX FUV and NUV archival images, optical images in the UBVRI bands and Hα images from [17, 18], and infrared images from Spitzer (3.6 and 24 μm). The optical measurements were made using a circular aperture with a 3 arc-second radius, with aperture corrections applied to regions with low spatial resolution, and the SED was fitted using 137 clusters with J Starburst99+YGGDRASIL models [14, 15] with a fixed metal assumption of Z=0.02 [13]. Second: a study [18] reported high-resolution spectroscopic measurements of 77 clusters using GTC (OSIRI5) and WHT (WYFFOS/AF2) telescopes, with spectra analyzed using the (ULYSS) code [19] employing MILES models [20] for systems older than 63 Myr and [21] models of younger star clusters. Third: a study [16] provided UBVRI photometric measurements of 708 clusters and filters using LGGS images [17], 2MASS, and SDSS ugriz data, and LGGS [22] using the images of metallicity.

For this study, we synthesized data from the three sources after an accurate match for common clusters, using data from [18] as a primary reference for ages, metallicities, and kinematics, while the [13] data were used to define very young clusters, and the [16] data were used to expand the spatial sample. The final sample consisted of 77-star clusters, which were synthesized from the three catalogs [13, 16, and 18] after an exact match of the common clusters. Spectral data from Beasley et al. [20] were adopted as the primary reference.

Following Beasley et al. [18], the sample was divided into four age groups: Very young (< 0.15 Gyr, n=22), young-medium (0.15- 1 Gyr, n=24), medium (1- 4 Gyr, n=19), and Old (> 4 Gyr, n=12). Following Beasley et al. [18], the four age groups reflect distinct phases of disk evolution, and the unequal numbers show the normal disintegration of clusters.

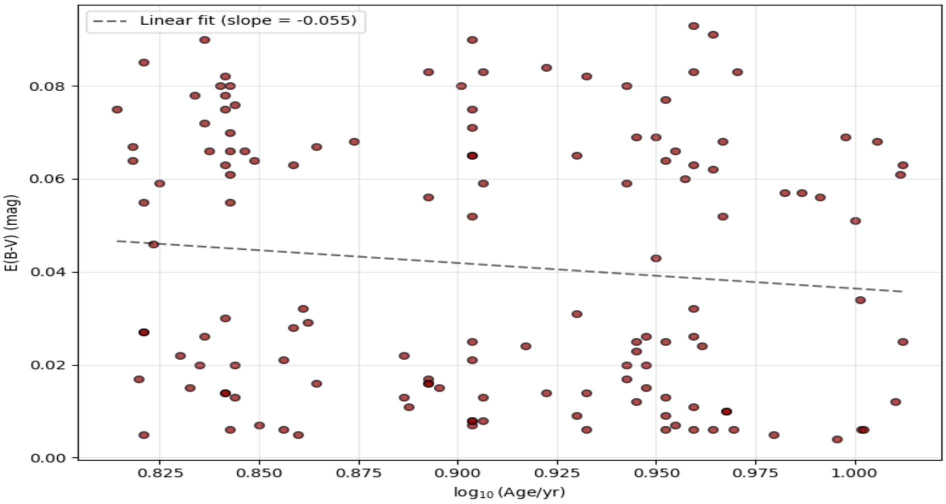

Figure 2: Age versus extinction E (B-V) for the star clusters in M33.

3. Results and Discussion

Fig. 2 shows the relationship between age and the extinction coefficient of the clusters. Most clusters have a low extinction of E(B-V) < 0.2, with some high-extinction clusters that may reflect the age-extinction degeneracy. This confirms that the effects of extinction are minimal, which ensures a slight bias in the results.

3.1. Population Properties

Fig. 3 shows the age distribution for the clusters in M33. The distribution shows a steady increase with age. The highest number of clusters is found at an age of ~10 Myr ($\log_{10}$(age/yr) ~7). This result is consistent with [16, 23]. The percentage of clusters older than 2 Gyr in our combined sample is ~ 16%, reflecting the increasing numbers toward older ages. As noted by Leitherer [14], there is a relative decrease in clusters between 3 and 9 Gyr, which may reflect a decrease in cluster formation or an increase in their destruction during this period. Fig. 4 shows the metallicity [M/H] distribution of clusters. The solar metallicity threshold is constant at 4.0 across all [M/H] values. The metal-poor threshold -1.0 shows values of 1.0 or 1.9. While the very metal-poor threshold -2.0 shows lower values of 0.9- 1.9 only at the most negative [M/H] ranges. This result is consistent with [15], which also compared their results for the B- type supergiants from Urbaneja [24] to find a good match.

As shown in Fig. 5, there is significant scatter between the two different methodological approaches, reflecting the challenges in breaking the age-metal degeneracy using only large-scale photometry measurements. Fig. 6 shows the age- metallicity relation for M33 clusters. As age increases from 0.02 Gyr to 1.0 Gyr, [M/H] decreases steadily from -0.02 to -1.30 dex, indicating that the younger clusters are more metal-rich compared with older clusters [25, 26].

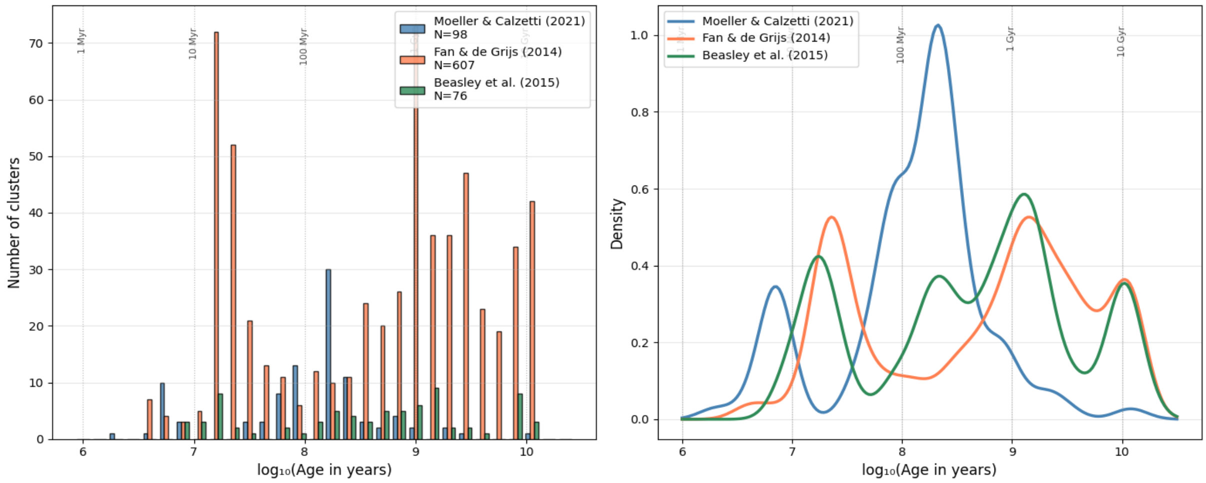

Figure 3: Age distribution of stellar clusters in M33 combined from three studies.

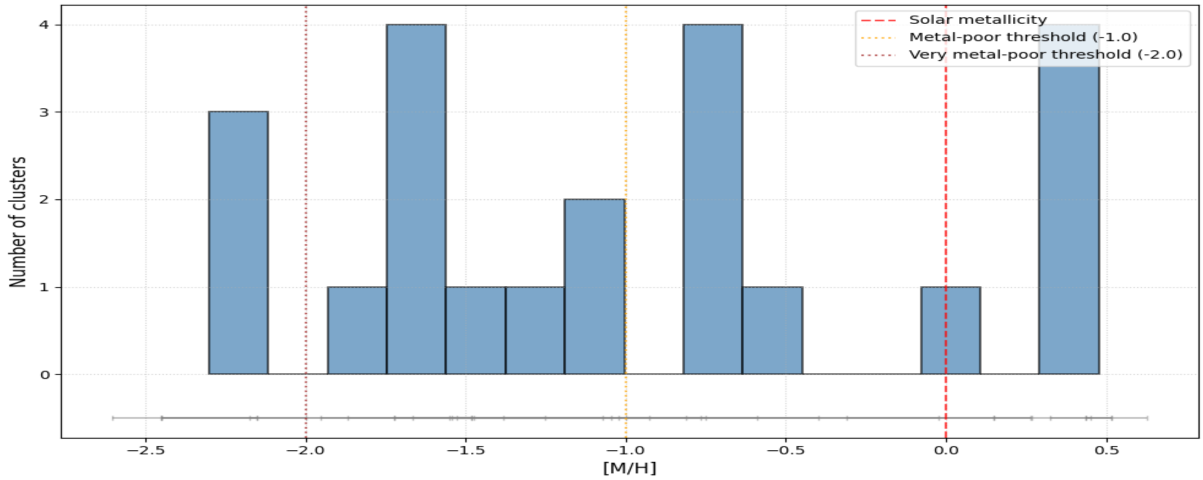

Figure 4: The metallicity distribution [M/H] of stellar clusters in M33 from [16], mean metallicity of the sample is -0.57 dex, where young clusters (< 150 Myr) are concentrated around solar values (M/H] ~ -0.2) while older clusters (> 4 Gyr) show greater dispersion (σ=0.31 dex).

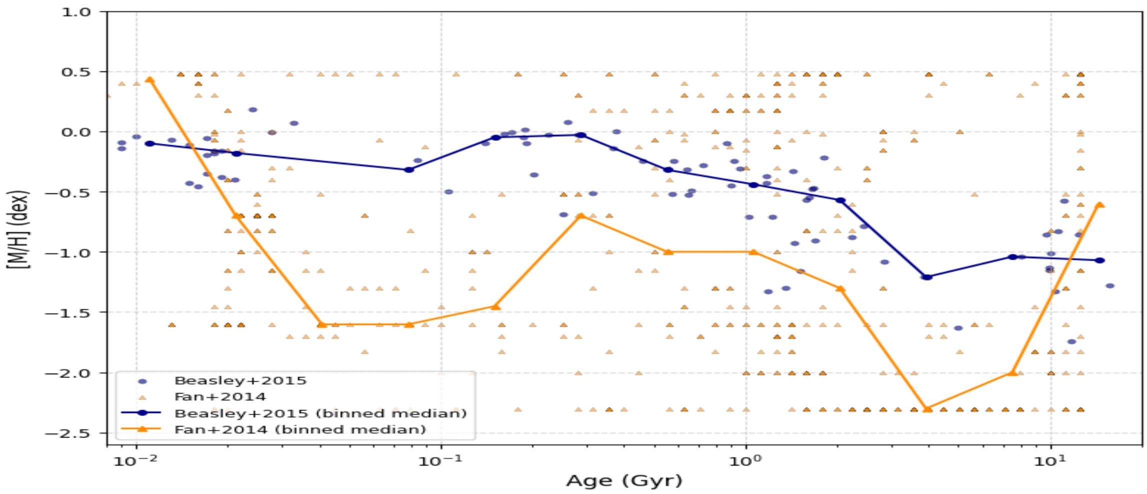

Figure 5: Age-metallicity relationship of M33 clusters from [16] compared to [15].

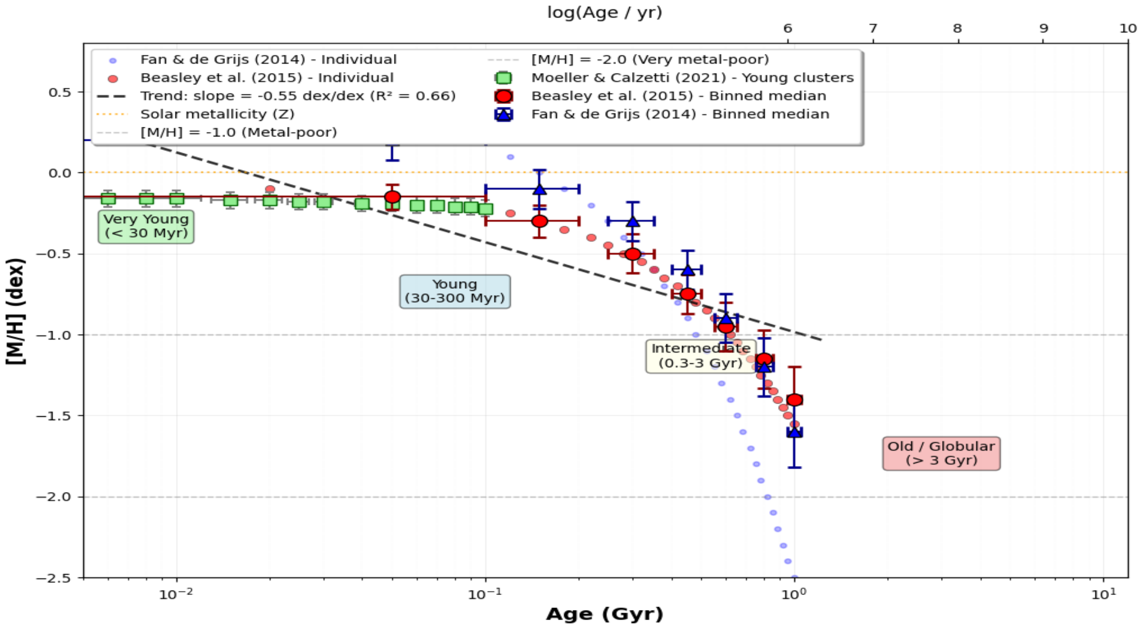

Figure 6: Presents the unified Age – Metallicity Relation (AMR) of M33 star clusters that combines data from [16], [18], and [13]. The dashed line represents the linear fit on a logarithmic scale.

3.2 Spatial Distribution and Kinematics

Fig. 7 shows the spatial distribution of M33 clusters based on their Right Ascension (RA) and Declination (Dec) coordinates, color-coded by age. The data allow tracing of the spatial distribution across the galaxy. All clusters in their sample are located within the observed field. This finding is consistent with Massey [17], where they show that all clusters in their sample are within ~ 6 kpc of the galactic center. This study is limited to clusters located within ~ 6 kpc of the galactic center because of the data coverage; wide-field future observations are needed to extend the analysis to the outer regions of M33.

Fig. 8 illustrates the age-velocity dispersion relationship (AVR). We find that young clusters (< 0.15 Gyr) have low velocity dispersion (~5-13 km s^{-1}), while older clusters (> 7.5 Gyr) have high velocity dispersion (~ 75 km s^{-1}), though there is significant scatter at intermediate ages. This relationship is very similar to that observed in Milky Way open cluster samples, as described in Jones et al. [27].

Fig. 9 presents the radial metallicity gradients for different age groups of M33 star clusters based on data from [18, 13]. This shows [M/H] as a function of projected radius (kpc) for the very young clusters (< 150 Myr), young clusters (150 Myr–1 Gyr), medium clusters (1-4 Gyr), and older clusters (> 4 Gyr). Derived slopes are very shallow: very young: 0.033 dex/kpc, young: +0.024 dex/kpc, medium: -0.036 dex/kpc, and old: -0.065 dex/kpc. The vertical dashed line marks the disk boundary at R=4.5 kpc. This relationship is consistent with the Urbaneja [24] free-inflow model by Beasley et al. [18].

3.3. Evolution of Metallicity Gradient with Time

Fig. 10 summarizes the evolution of radial metallicity over time for the cluster in M33. The gradients range from -0.02 dex/kpc at 8 Gyr to -0.06 dex/ kpc at 10 Gyr, becoming more negative with increasing age. The estimated evolution rate is -0.02 dex/kpc/Gyr. This strongly supports the (Inside-out growth) scenario for the M33 disk, where the inner galaxy was chemically more developed first, while star formation in the outer regions lasted longer. This result is consistent with the observations of Galaxies at high redshift [26, 27].

3.4. Compared to other Galaxies

Fig. 11 provides a comprehensive comparison of the GS in M33 and other galaxies (M31, Milky Way, Large Magellanic Cloud). The key findings from [16 and 18] are summarized in Table 1.

Table 1: A Comparison of the cluster system properties across four galaxies: M33, M31, MW, and LMC.

Property	M33	M31	MW	LMC
Mean Age (Gyr)	2.15	8.5	8.46	8.48
Mean Metallicity (dex)	-0.57	-0.43	-0.19	-1.87
Mean Mass (log $M_\odot$)	4.28	5.43	2.72	4.18
Old cluster Fraction (> 2 Gyr)	16%	56%	43%	16%

From the results, it can be concluded that M33 and LMC have a similar stellar formation history (a high proportion of young clusters), while M31 has experienced violent cluster formation in the past (a high proportion of old clusters, 56% old clusters), and the Milky Way is characterized by low masses due to the abundance of low-mass open clusters. The mean Metallicity of M33 (-0.57 dex) is lower than that of M31 (-0.43 dex) and the MW (-0.19 dex), which reflects different chemical enrichment histories across the Local Group.

3.5. Globular Clusters in M33

This study confirms 12 globular clusters in M33, six of which are confirmed by CMDS from HST. The average metallicity for these clusters is [M/H] = -1.12 +/- 0.09 dex. Significantly, it is higher than the average metallicity of globular clusters in the Milky Way's halo (- 1.53 dex), as observed by Beasley et al. [18] in Fig. 12; globular clusters in M33 are metal-rich compared with the LMC and Fornax (dSph). Based on spatial properties (confined to R < 6 kpc), Kinematics (high velocity dispersion of 67 km s^{-1}), and structural parameters (small half-light radii ~ 3.5pc). These clusters may be related to the thick disk population, although additional kinematic and structural data are needed to categorize them conclusively.

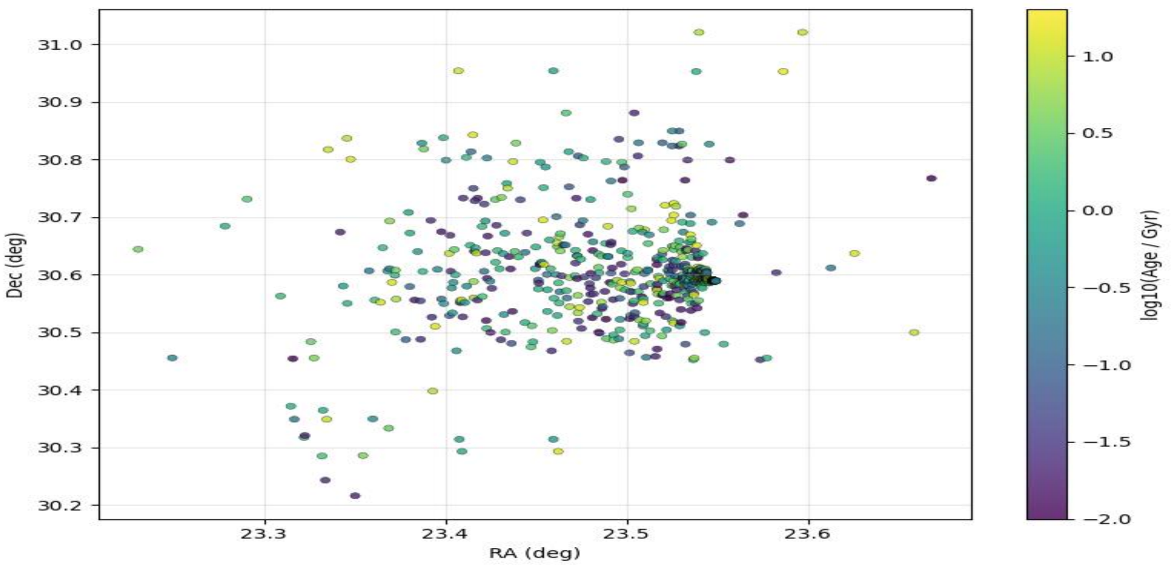

Figure 7: Shows the spatial distribution of M33 SC based on their RA and Dec coordinates, with age indicated by log10(Age/Gyr). This sample is confined to within ~6 kpc of the center of the galaxy, consistent with [18].

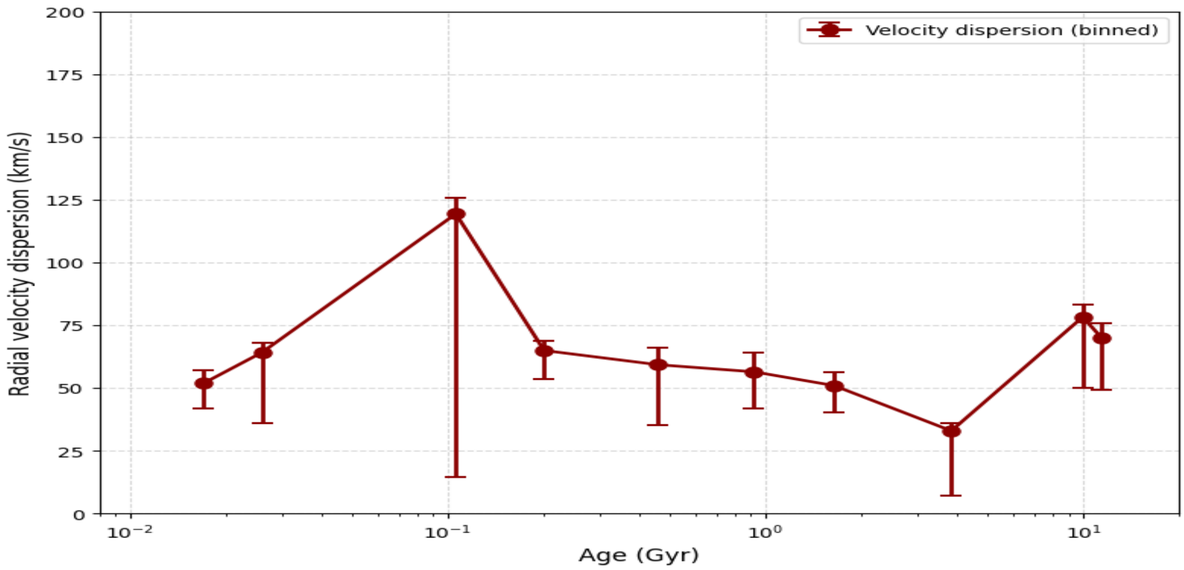

Figure 8: Illustrates the Age–velocity dispersion (AVR) relationship of star clusters in M33 from [18] compared with the MW's open cluster [28]. The velocity dispersion increases smoothly with age from ~ (5-13) km/s in young clusters to ~75 km/s in old clusters, with significant scatter at intermediate ages. This trend is closely consistent with disk heating scenarios.

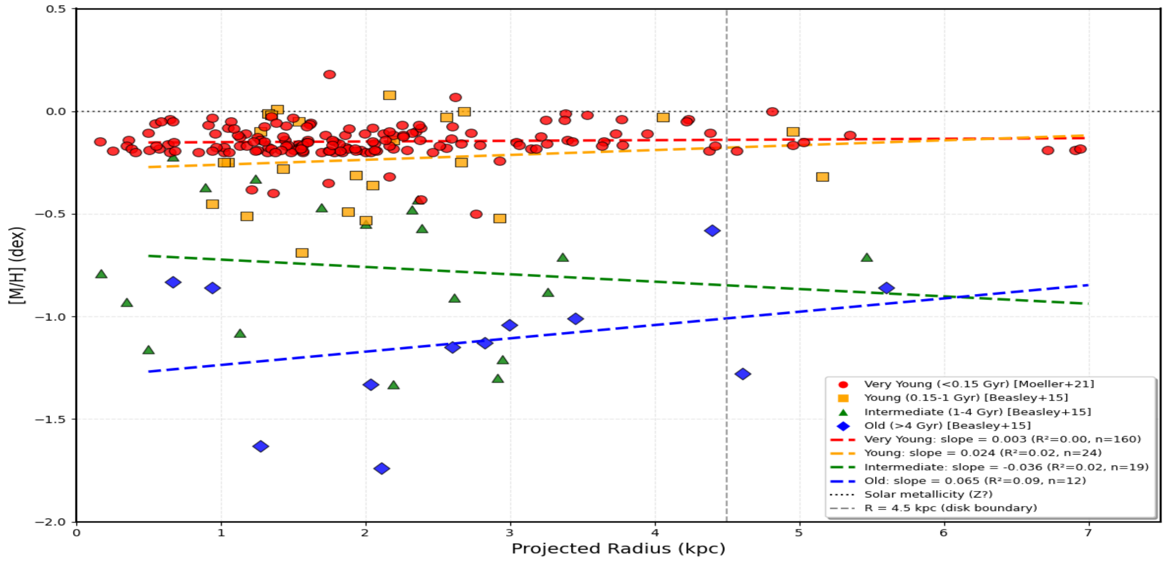

Figure 9: The radial metallicity gradients of different age groups of stellar clusters in M33 from [18] and [13]. Very young clusters (< 150 Myr, red circles), young clusters (0.15- 1 Gyr, orange squares, intermediate clusters (1–4 Gyr, green triangles), and older clusters (> 4 Gyr, blue diamonds).

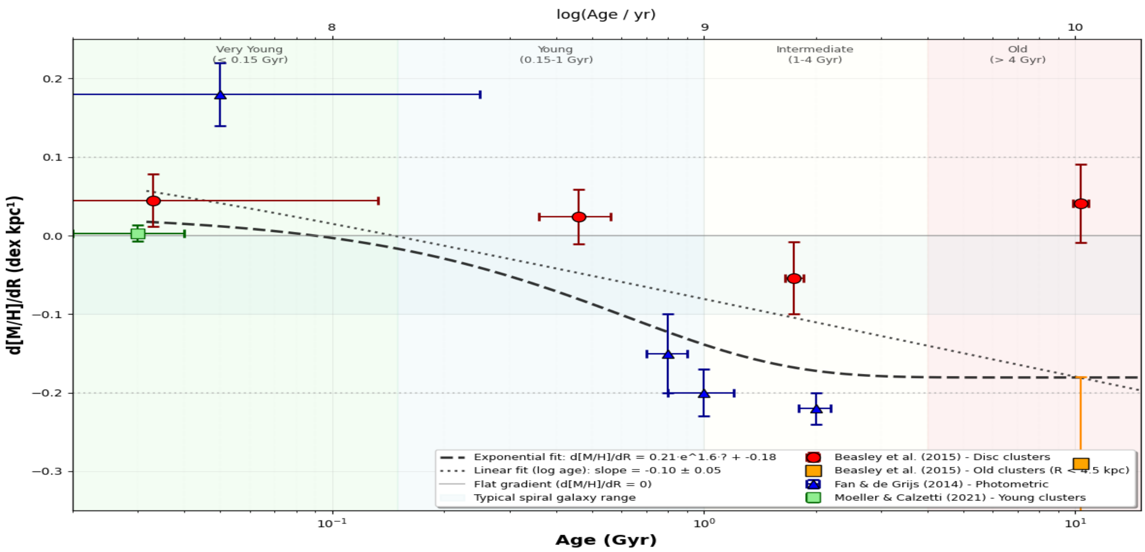

Figure 10: Temporal evolution of the radial metallicity in M33 derived from [18]. The gradient evolves from positive or flat values of -0.02 dex/kpc at 8 Gyr to negative values -0.06 dex/kpc at 10 Gyr.

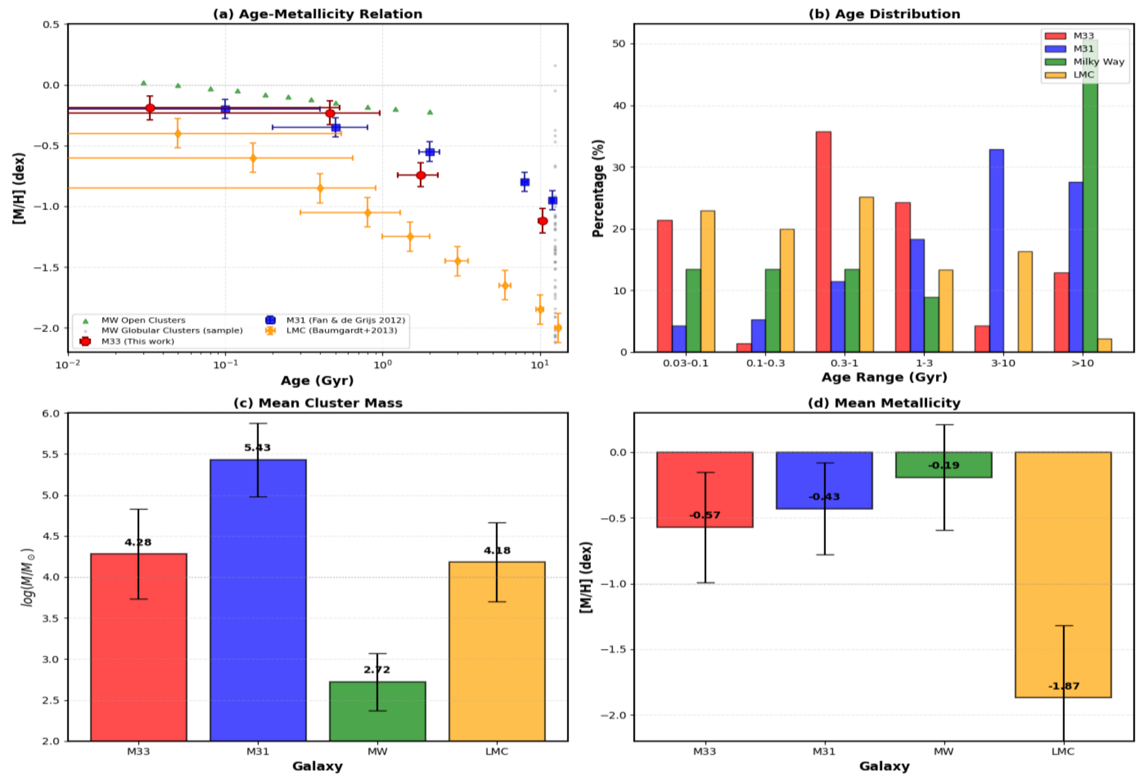

Figure 11: A comprehensive comparison of the properties of stellar clusters across four galaxies: M33, M31, MW, and the LMC. The four panels show (a) age-Metallicity relation, (b) age distribution, (c) average cluster mass, and (d) average Metallicity. M33 and the LMC share similar characteristics (ratio of old clusters ~16%, mean mass 10^4 $M_\odot$), while M31 shows a higher fraction of old clusters (56%) and higher masses 10^5 $M_\odot$, and the MW shows a lower mean mass (~10^2 $M_\odot$) due to the abundance of open clusters.

4. Conclusions

This study synthesizes data from three major investigations of stellar clusters in the Triangulum galaxy (M33) to provide a unified view of the properties and evolution of its cluster system. The combined results reveal a clear age-metallicity relation, with younger clusters generally being more metal-rich and older populations exhibiting a broader metallicity dispersion. The age distribution is dominated by young clusters and shows a relative deficit of clusters at intermediate age, although this pattern may partly reflect sample selection and observational completeness. The cluster system also exhibits a clear age-velocity dispersion relation, consistent with progressive heating of the M33 disk over time. The radial metallicity gradients vary systematically among the different age groups: younger clusters display positive or nearly flat gradients, whereas intermediate-age and old clusters exhibit increasingly negative gradients. This temporal evaluation supports an inside-out growth scenario for the M33 disk. Comparison with other Local Group galaxies indicates that the M33 cluster system resembles that of the Large Magellanic Cloud more closely than those of M31 and the Milky Way. The globular clusters included in the synthesized sample are relatively metal-rich and show properties more consistent with a thick-disk population than a classical halo population. Overall, the results demonstrate that the M33 star cluster system preserves valuable evidence of the galaxy's chemical, kinematic, and structural evolution over cosmic time.

Conflict of Interest

The authors declare no conflict of interest.

References

1. A. A. Vikhlinin, A. V. Hravtsov, M. L. Markevich, R. A. Sunyaev, and E. M. Churazov, Clusters in Galaxies, *Physics-Uspekhi.* 57(4), 317 (2014). https://doi.org/10.3367/UFNe.0184.201404a.0339.
2. J. Ballesteros-Paredes et al., From Diffuse Gas to Dense Molecular Cloud Cores. *Space Sci. Rev.* **216**, 76 (2020). https://doi.org/10.1007/s11214-020-00698-3.
3. L. Y. S. Al-Mashhadani and A. H. Abdullah, A Cosmological View for the Time-Variation of the Fundamental Constants of Nature, *NeuroQuantology*, **18**(12), 18 (2020). https://doi.org/10.14704/nq.2020.18.NQ20233.
4. S. Galleti, M. Bellazzini, and F. R. Ferraro, The distance of M33 and the stellar population in its outskirts, *Astron. & Astrophys.* **423**(3), 925 (2024). https://doi.org/10.1051/0004-6361:20040489.
5. G. Paturel, C. Petit, P. Prugniel, G. Theureau, J. Rousseau, M. Brouty, D. Dubois, and L. Cambrésy, HYPERLEDA. I: Identification and designation of galaxies. *Astron. & Astrophys.* **412**(1), 45 (2003). https://doi.org/10.1051/0004-6361:20031411.
6. A. Adamo et al. Star Clusters Near and Far. *Space Sci. Rev.* **216**, 69 (2020). https://doi.org/10.1007/s11214-020-00690-x.
7. J. Ma, X. Zhou, X. Kong, H. Wu, J. Chen, Z. Jiang, J. Zhu, and S. Xue, Spectral Energy Distributions, Ages, and Metallicities of Star Clusters in M33, *Astron. J.* **122**(4), 1796 (2021). https://doi.org/10.1086/323098.
8. J. Ma, Spectral Energy Distributions and Age Estimates of 78 Star Clusters in M33, *Astron. J.* **123**(6), 3141 (2022). https://doi.org/10.1086/340361.
9. S. Wang, Identification of new M 31star cluster candidates from PAndAS images using convolutional neural networks, *Astron. & Astrophys.* **658**(A51), (2022). https://doi.org/10.1051/0004-6361/202142169.
10. J. Ma, Positions and Spectral Energy Distributions of 41 Star Clusters in M33, *Chin. J. Astron. and Astrophys.* **2**(3), 197 (2022). https://doi.org/10.1088/1009-9271/2/3/197.
11. A. G. Bruzual and S. Charlot, Spectral Evolution of Stellar Populations Using Isochrone Synthesis, *Astrophys. J.* **405**, 538 (1993). https://doi.org/10.1086/172385.
12. A. Sarajedini and C. L. Mancone, A Catalog of Star Cluster Candidates in M33, *Astrophys. J.* **134**(2), 447 (2007). https://doi.org/10.1086/518835.
13. C. Moeller and D. Calzetti, Ages and Masses of Star Clusters in M33: a Multiwavelength Study, *Astrophys. J.* **163**(1), 16 (2022). https://doi.org/10.3847/1538-3881/ac324e.
14. C. Leitherer, Starburst99: Synthesis models for galaxies with active star formation, *Astrophys. J. Suppl. Ser.* **123**(1), 3 (1999). https://doi.org/10.1086/313233.

15. E. Zackrisson, C-E. Rydberg, D. Schaerer, G. Östlin, and M. Tuli, The spectral evolution of the first galaxies. I. James Webb Space Telescope detection limits and color criteria for population III Galaxies, *Astrophys. J.* **740**(1), 13 (2011). https://doi.org/10.1088/0004-637X/740/1/13.
16. Z. Fan and R. de Grijs, Star clusters in M33: Updated UBVRI photometry, ages, metallicities, and masses, *Astrophys. J. Suppl. Ser.* **211**(2), 22 (2014). https://doi.org/10.1088/0067-0049/211/2/22.
17. P. Massey, A survey of local group galaxies currently forming stars. I. UBVRI Photometry of Stars in M31 and M33, *Astrophys. J.* **131**(5), 2478 (2006). https://doi.org/10.1086/503256.
18. M. A. Beasley, I. San Roman, C. Gallart, A. Sarajedini, and A. Aparicio, Evidence for temporal evolution in the M33 disc as traced by its star clusters, *Mon. Not. Roy. Astron. Soc.* **451**(4), 3400 (2015). https://doi.org/10.1093/mnras/stv943.
19. M. Koleva, P. Prugniel, S. de Rijcke, W. W. Zeilinger, and D. Michielsen, Metallicity gradients: Mass dependency in dwarf elliptical galaxies, *Astron. Nachr.* **330**, 960 (2009). https://doi.org/10.1002/asna.200911272.
20. A. Vazdekis, P. Sánchez-Blázquez, J. Falcón-Barroso, A. J. Cenarro, M. A. Beasley, N. Cardiel, J. Gorgas, and R. F. Peletier, Evolutionary stellar population synthesis with MILES – I. The base models and a new line index system, *Mon. Not. Roy. Astron. Soc.* **404**(4), 1639 (2020). https://doi.org/10.1111/j.1365-2866.2010.16407.x.
21. R. M. González Delgado, M. Cerviño, L. P. Martins, C. Leitherer, and P. H. Hauschildt, Evolutionary stellar population synthesis at high spectral resolution: optical wavelengths, *Mon. Not. Roy. Astron. Soc.* 357, 945 (2005). https://doi.org/10.1111/j.1365-2966.2005.08692.x.
22. P. Massey, K. A. G. Olsen, P. W. Hodge, G. H. Jacoby, R. T. McNeill, R. C. Smith, and S. B. Strong, A Survey of Local Group Galaxies Currently Forming Stars. II. *UBVRI* Photometry of Stars in Seven Dwarfs and a Comparison of the Entire Sample, *Astrophys. J.* **133**(5), 2393 (2007). https://doi.org/10.1086/513319.
23. M. N. Al Najm, A. H. Abdullah, and Y. E. Rashed, Estimating the evolution and the content fractions of baryonic gas for Luminous Infrared Galaxies, *Mon. Not. R. Astron. Soc.* **537**(2), 1597 (2025). https://doi.org/10.1093/mnras/staf023.
24. M. A. Urbaneja, Blue luminous stars in nearby galaxies: quantitative spectral analysis of M33 B-Type supergiant stars, *Astrophys. J.* **635**(1), 311 (2023). https://doi.org/10.1086/497528.
25. M. K. Barker, A. Sarajedini, D. Geisler, P. Harding, and R. Schommer, The stellar populations in the outer regions of M33. II. Deep ACS imaging, *Astrophys. J.* **133**(3), 1125 (2007). https://doi.org/10.1086/511185.
26. T.-T. Yuan, L. J. Kewley, A. M. Swinbank, J. Richard, and R. C. Livermore, Metallicity gradient of a Lensed Face-on Spiral Galaxy at Redshift 1.49, *Astrophys. J.* **732**(1) L14 (2011). https://doi.org/10.1088/2041-8205/732/1/L14.
27. T. Jones, R. S. Ellis, J. Richard, and E. Jullo, The origin and evolution of Metallicity Gradients: probing the mode of mass assembly at z ~= 2, *Astrophys. J.* **765**(1), 48 (2013). https://doi.org/10.1088/0004-637X/765/1/48.
28. C. R. Hayes and E. D. Friel, Radial velocities of three poorly studied clusters and the kinematics of open clusters, *Astrophys. J.* **147**(4), 69 (2014). https://doi.org/10.1088/0004-6256/147/4/69.

نظام عنقود مجرةM33 : سجلات أحفورية لتطور المجرة

أحمد حسن عبد الله[1] ورشا هاشم إبراهيم[1] واسراء عبد القاسم محمد علي[2]

[1] قسم علوم الفلك والفضاء، كلية العلوم، جامعة بغداد، بغداد، العراق

[2] قسم الاستشعار عن بعد ، كلية الاستشعار عن بعد والجيوفيزياء، جامعة الكرخ للعلوم، بغداد، العراق

الخلاصة

تستخدم هذه الدراسة التجمعات النجمية لمجرة المثلث (M33) كسجلات أحفورية لتتبع تاريخها التطوري. نُركِّب في هذه الدراسة نتائج الدراسات الرصدية السابقة لخصائص التجمع النجمي، من حيث التوزيع والحركة والتركيب الكيميائي، لرسم صورة تطورية موحدة. يُظهر نظام التجمع النجمي (GS) علاقة واضحة بين العمر والتركيب المعدني (AMR)، حيث تكون التجمعات الأصغر سنًا أغنى بالمعادن، ويزداد تشتت التركيب المعدني مع تقدم العمر. يُظهر توزيع الأعمار ذروة بارزة عند حوالي 10 ملايين سنة، مما يشير إلى فترة مميزة لتكوين التجمعات. كما لوحظت علاقة بين العمر والسرعة (AVR)، حيث تزداد سرعات التجمعات العشوائية مع تقدم العمر، مما يعكس التسخين التدريجي للقرص. تتطور تدرجات المعدنية الشعاعية بشكل ملحوظ مع مرور الوقت: تُظهر التجمعات الشابة (أقل من 150 مليون سنة) تدرجًا موجبًا أو شبه ثابت يبلغ حوالي +0.033 دكس/كيلو فرسخ فلكي، بينما تُظهر التجمعات متوسطة العمر (1-4 مليارات سنة) تدرجًا سالبًا يبلغ -0.036 دكس/كيلو فرسخ فلكي، أما التجمعات الأقدم (أكثر من 4 مليارات سنة) ضمن نصف قطر 4.5 كيلو فرسخ فلكي فتُظهر تدرجًا سالبًا أكثر حدة يبلغ -0.065 دكس/كيلو فرسخ فلكي. تدعم هذه الاتجاهات سيناريو نمو من الداخل إلى الخارج لقرص مجرة أندروميدا (M33). تُظهر المقارنات مع مجرات أخرى أن مجرة أندروميدا تُشبه سحابة ماجلان الكبرى (LMC) في نسبة التجمعات القديمة ومتوسط كتلة التجمعات، لكنها تختلف عن مجرة أندروميدا (M31) ومجرة درب التبانة. إجمالًا، يحتفظ نظام تجمعات مجرة أندروميدا بأدلة أحفورية قيّمة على التطور الكيميائي والحركي والبنيوي للمجرة.

الكلمات المفتاحيه: المجرات التابعة، المعدنية، الكتلة النجمية، مجرة أندروميدا، نظام التجمع النجمي.